Available online at www.sciencedirect.com
SCIENCE DIRECT
Journal of Power Sources 155 (2006) 358–363
JOURNAL OF POWER SOURCES
www.elsevier.com/locate/jpowsour

Evaluation of copper oxide thin films as electrodes for microbatteries

E.A. Souza [a], R. Landers [a], L.P. Cardoso [a], Tersio G.S. Cruz [b], M.H. Tabacniks [c], A. Gorenstein [a,*]

[a] *Applied Physics Department, Physics Institute, UNICAMP, CP 6165, CEP 13083-970 Campinas, SP, Brazil*
[b] *Telecommunication Technological Division, CESET/UNICAMP, CEP 13484-370 São Paulo, SP, Brazil*
[c] *Physics Institute, USP, CP 66318, CEP 05389-970 São Paulo, SP, Brazil*

Received 8 March 2005; received in revised form 21 April 2005; accepted 21 April 2005
Available online 20 June 2005

Abstract

In this work, copper oxide thin films have been evaluated for use as electrodes in thin film batteries. The films were deposited by dc sputtering at low power, in order to produce nanoparticulated films. Samples were deposited onto unheated or heated (420 °C) substrates. Both kind of samples are nanoparticulated, with distinct grain sizes, and amorphous. The potential profiles and cycling capacity in lithium electrolyte were investigated and are similar to those obtained for copper oxide in powder form. The discharge capacity for samples deposited onto heated substrates depends on the previous treatment of the samples, and the stabilized capacity values are higher than for the samples deposited without intentional heating of the substrates, and suitable for use in lithium-ion microbatteries.

Keywords: Copper oxide; Reactive sputtering; Thin films; Microbatteries

1. Introduction

Cupric oxide has been pointed out as a suitable compound for cathodes in lithium batteries [1] and, more recently, as alternative materials for anodes in lithium-ion batteries [2,3]. The lithium reaction with these materials cannot be classified as a classical intercalation reaction, since it promotes a whole rearrangement of the oxide structure. As a consequence of the lithium reaction, the original particles are subdivided in smaller ones, and metallic copper agglomerate as metal inclusions in the system. Li_2O is formed in the process. Surprisingly, the reactions are quite reversible, and the original oxide can be partially recovered. Most of the metal oxide materials already investigated are in powder form and very few systems have been investigated in thin film form [4,5].

In this work, copper oxide thin films were deposited by reactive dc sputtering at low power, in order to produce nanoparticulated films. Their behavior with respect to lithium reactions is presented.

2. Experimental

The copper oxide films were deposited by dc sputtering from a copper target in an O_2 + Ar atmosphere. The flow of the gases was controlled by two mass flowmeters, and was fixed at 55.0 standard cubic centimeter (sccm, Ar) and 5.0 sccm (O_2), The pressure under deposition was 9.4×10^{-3} mbar and the dc power was 4 W. The substrates (indium–tin oxide, ITO, onto glass or Si) were either unheated, or intentionally heated to 420 °C.

Thickness of the films were ∼210 nm (samples deposited onto unheated substrates) and ∼120 nm (samples deposited onto heated substrates), as measured with an Alpha-Step profilometer. The deposition time was 120 min corresponding to the deposition rate of 1.75 and 0.99 nm min^{-1}, respectively.

The presence of crystalline phases was investigated by X-ray diffraction under grazing incidence geometry with Cu

* Corresponding author. Tel.: +55 19 37885411; fax: +55 19 37885376.
E-mail address: annette@ifi.unicamp.br (A. Gorenstein).

0378-7753/$ – see front matter © 2005 Elsevier B.V. All rights reserved.
doi:10.1016/j.jpowsour.2005.04.014

Kα radiation in the X Pert MRD Philips equipment. Surface morphology was examined with an atomic force microscope (AFM, Topometrix TMX 2000 SPM equipment). Grain size and root mean square surface roughness were determined from AFM images within an area of 1.0 μm × 1.0 μm. Cu and O contents were obtained by Rutherford scattering spectroscopy (RBS) using a 2.2 MeV He^+ beam. The chemical state of the metal was analyzed by X-ray photoelectron spectroscopy (XPS).

Electrochemical cells with the copper-oxide films as the working electrode and two Li metal foils as the reference and counter electrode were used for electrochemical measurements. The electrolyte was 1 M $LiClO_4$ in propylene carbonate. Chronopotentiometric experiments were performed from rest potential to 1 V versus Li, using a current density of 2.0 μA cm^{-2}, by means of a multipotentiostat (VMP system, Biologic) operating in the galvanostatic mode. During the experiments, the cell was maintained inside an Ar dry-box.

3. Results and discussion

Fig. 1 presents 1.0 μm × 1.0 μm AFM micrographies for samples deposited without intentional heating of the substrate (Fig. 1a) and samples deposited onto heated substrates (Fig. 1b). The inset of the figures presents the corresponding typical line profiles. It is clear from the figures that the films consists of uniformly distributed grains, and that heating of the substrate induces the formation of larger grains, as has been already observed by other authors [6]. The increase

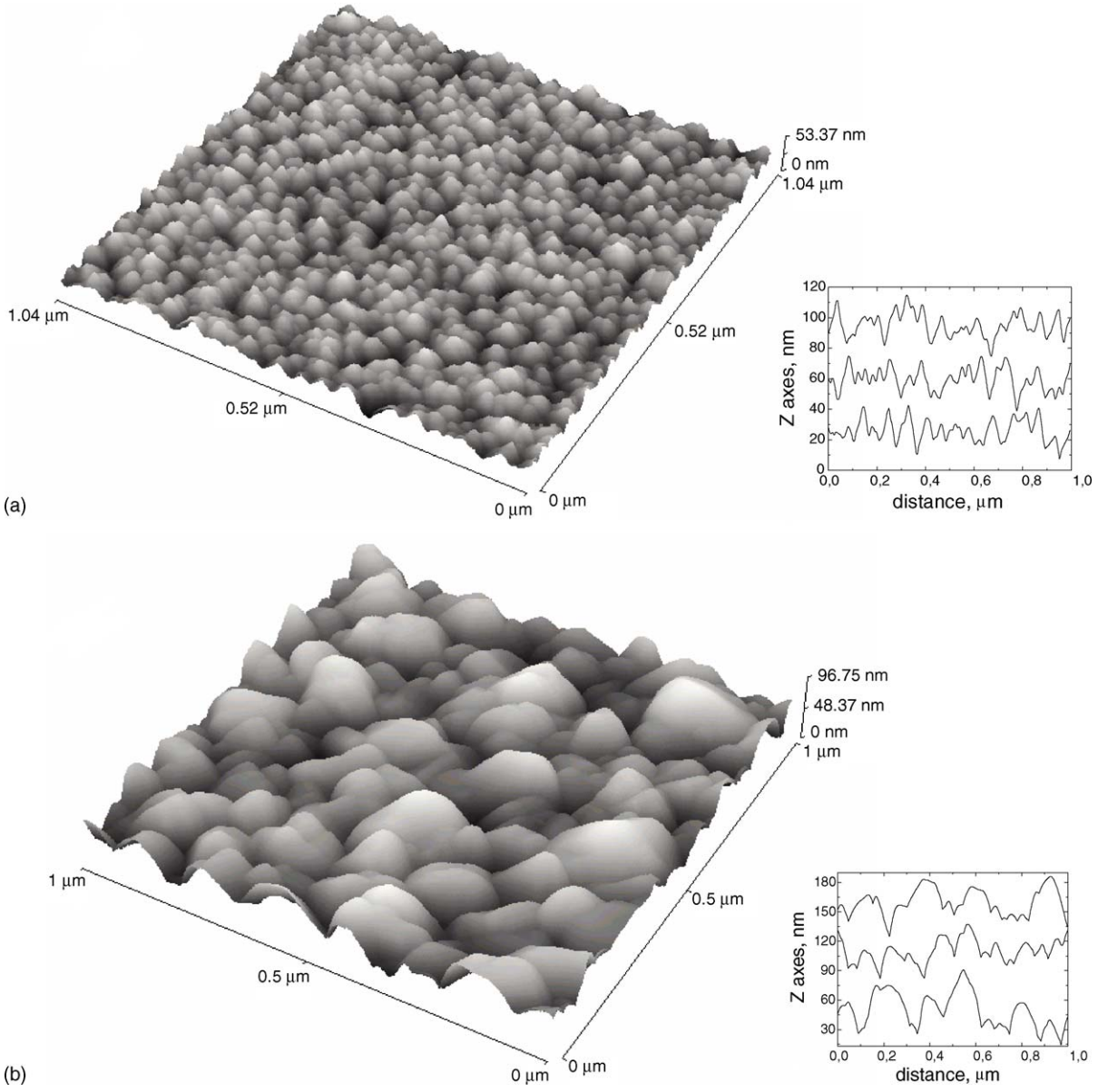

Fig. 1. 1.0 μm × 1.0 μm AFM micrographies for samples deposited without intentional heating of the substrate (a) or for samples deposited onto heated substrates (420 °C, b). The inset of the figures presents the corresponding line profiles.

of grain size with temperature was described by Thornton, who proposed the well-known structure-zone model [7]. In the present study, the films are located at (or very close to) the low temperature zone (Zone 1, in which $T/T_m < 0.3$, T being the substrate temperature and T_m the coating material melting point). The main growth mechanism for films deposited at temperatures in the Zone 1 range is shadowing, and an increase in grain size is expected with the increase of T/T_m. The mean grain size for the sample deposited onto unheated substrate is ∼50 nm and the value for the other sample is ∼127 nm. The root mean square (RMS) roughness, estimated from these AFM micrographs, is 7.5 and 16.6 nm, respectively.

The X-ray diffraction experiments carried out at grazing angles did not show any diffraction peaks, indicating the absence of long-range order, probably due to the low dc sputtering voltage.

Fig. 2 presents a characteristic RBS spectrum and the corresponding fitting curve, obtained by using the RUMP program [8]. The substrate was Si, and the film was deposited onto heated substrate. Only copper and oxygen were identified as the elements present in the film, without any indication of contamination. From this data the overall composition is calculated to be $Cu_{1.1}O$ and the calculated density is 4.9 g cm^{-3} (sample deposited onto heated substrate). This result indicates that the copper is present in the sample mainly in the Cu^{2+} state, with some copper metal contamination (unreacted metal).

This is in accordance with the XPS data. Fig. 3a shows the O1s XPS spectra, for both samples. The peak positions were obtained by fitting the XPS spectra with a Gaussian–Lorentzian mixed function. The main peak energy for the sample deposited with intentional heating of the substrate has a binding energy of 529.4 eV, consistent with the presence of CuO, since for this compound the O1s is present

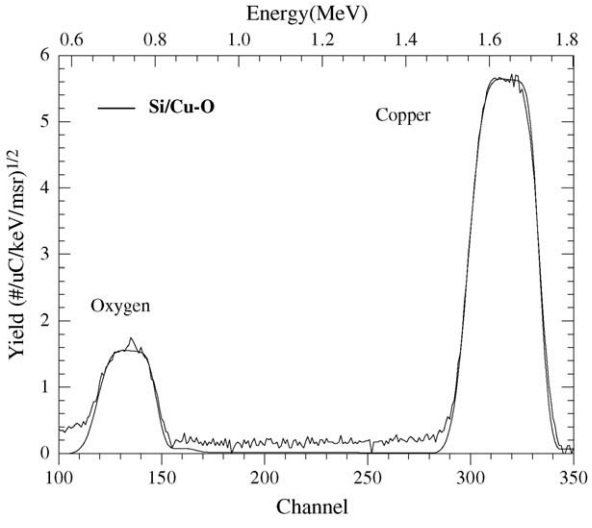

Fig. 2. RBS spectrum, and the corresponding fitting curve, for a sample deposited onto heated substrate.

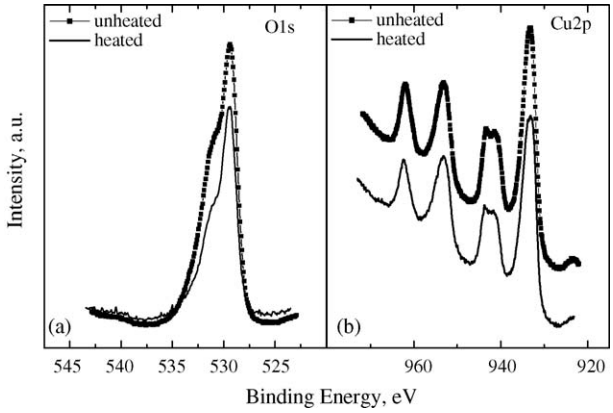

Fig. 3. (a) O1s XPS spectra and (b) Cu2p XPS spectra.

at binding energies in the interval 529.0–530.0 eV [9–11]. Two other peaks are present at higher energies, at 531.1 and 532.9 eV. The O1s line for Cu_2O is located at 530.0–531.0 eV, so these peaks could be attributed to contamination, such as hydroxides or organic compounds [10–13]. The main peak energy for the sample deposited without intentional heating of the substrate has a binding energy of 529.3 eV, which is also consistent with the presence of CuO.

Fig. 3b shows the Cu 2p3/2 XPS spectra. The main peak energy for the sample deposited with and without intentional heating of the substrate has a binding energy of 933.6 and 933.3 eV, respectively, and a satellite located at higher binding energies (9 eV), which is a fingerprint for the presence Cu^{2+} species (CuO compound) [9–11]. For the sample deposited onto heated substrate, the fitting process also indicates the presence of a shoulder located at 932.4 eV that could be indicative of the presence of Cu^0 in this sample [14].

Fig. 4a presents the voltage–composition curves for the first discharge and subsequent charge process. The data are relative to samples deposited without intentional heating of the substrate. The voltage–composition curve is similar to the curves observed for particulated CuO or Cu_2O [4]. The initial discharge profile shows an initial abrupt potential decrease from open circuit potential up to ∼2.5 V versus Li^+/Li, followed by a potential decrease presenting a first ill-defined plateau centered at ∼2.3 V versus Li^+/Li and two other plateaus centered at ∼1.4 V versus Li^+/Li and 1.2 V versus Li^+/Li.

The electrochemical behavior of copper oxide in lithium-containing electrolytes has been extensively studied, and a very large number of reactions have been proposed, in order to explain the features observed in, e.g., chronopotentiometric experiments. The reaction scheme is still controversial, probably due to the complexity of the system and the different methods of obtained of the starting material. Our cathode material was obtained by a thin film physical deposition technique and this kind of electrode, for the best of our knowledge, has not been previously studied. In particular, the plateau around 2.3 V versus Li^+/Li is not always observed in chronopotentiometric experiment, particularly in the first dis-

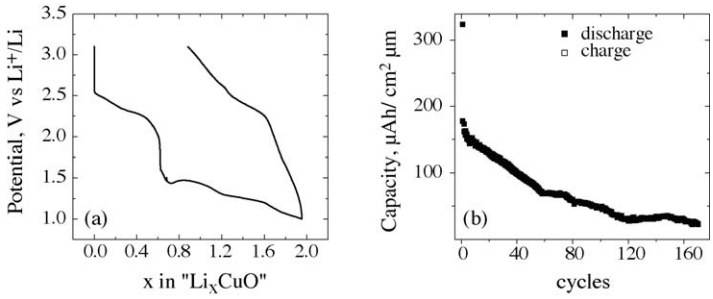

Fig. 4. (a) Voltage–composition curves, for the first discharge and first charge process, (b) capacity as a function of cycling. The sample was deposited without intentional heating of the substrate.

charge process [15,16]. Recently, a very detailed study allied electrochemical experiments with physical techniques as in situ X-ray diffraction and transmission electron microscopy [17]. For the potential region from open circuit to the plateau around 2.1 V versus Li^+/Li, the authors did not observe alteration of the structure of the starting material, and suggests the gradual reduction of Cu(II) in Cu(I) and oxygen vacancies creation in accordance with the reaction:

$$CuO + xLi^+ + xe^- \rightarrow [Cu^{II}_{1-x}Cu^{I}_{x}]O_{1-x/2} + \frac{x}{2}Li_2O \quad (1)$$

Our sample reacted, in this potential range, with 0.5 Li ions per mole of compound, which is compatible with this reaction scheme. The above-cited authors also observed an electrochemical plateau around 1.6 V versus Li^+/Li, which has been attributed to a physical phase transition (the disintegration of the initial copper oxide platelets into smaller copper oxide nanoparticles) [17]. Other authors, based on the AFM analysis of the surface of thin film electrodes, suggested the formation of a solid electrolyte interface (SEI), arising from reactions with the electrolyte [5]. In the present study a different electrolyte has been used and the plateau above 1.5 V versus Li^+/Li is very ill defined.

Several authors [1,17] agree that the 1.4 V versus Li^+/Li plateau arises from the reduction of copper oxide into copper nanograins and formation of Li_2O, in accordance with the reaction:

$$Cu_2O + 2Li^+ + 2e^- \rightarrow 2Cu + Li_2O \quad (2)$$

Electrochemical quartz crystal microbalance (EQCM) experiments [4] suggested the simultaneous formation of lithium carbonate. In what concerns the 1.2 V versus Li^+/Li plateau, the EQCM experiments [4] did not show significant mass changes in this potential region, and pure capacitive behavior or reactions involving the SEI can be suggested.

In the potential range from open circuit to 1.0 V versus Li^+/Li this sample reacts with 2 Li ions per mole of compound, corresponding to capacities of 324 $\mu Ah\,cm^{-2}\,\mu m^{-1}$ ($\sim$660 $mAh\,g^{-1}$); this value correspond to 76% of the theoretical value for the CuO/Cu reduction process (426 $\mu Ah\,cm^{-2}\,\mu m^{-1}$ or 670 $mAh\,g^{-1}$). On the first charge process, and for the subsequent cycles, the profile is altered indicating irreversible structural-composition changes on the electrode [15]. The capacity loss on the first discharge/charge cycle is $\sim$50%.

The substrate used in these experiments is glass covered with ITO. Lithium ion insertion into ITO has been studied previously [18,19] and the electrochemical activity of these electrodes, in our experience, is very dependent on the transparent/conducting thin film deposition parameters, since normally these materials are optimized in what concerns their optical transparency and electronic resistivity [20]. In many cases the influence of the substrate on the electrochemical performance of thin film electrodes is not taken into account, due to the barrier effect of the compact thin film. In the present case, however, the original copper oxide compact film can suffer important modifications (formation of smaller grains, either of copper oxide or metallic copper) and the possibility of direct contact of the substrate with the electrolyte cannot be discarded. The lithium reaction with ITO occurs at potentials below 1.5 V versus Li^+/Li, and could mask the copper oxide reaction scheme, adding further complexity to the system. The measured capacity of our substrate is 0.02 $\mu Ah\,cm^{-2}\,\mu m^{-1}$ (first cycle) and an order of magnitude lower for the second cycle. This value is much lower than the measured capacity of the substrate covered with the copper oxide film. However, if the substrate is participating in the reaction, a decrease in its conductivity should be expected, and could be a possible reason for the decrease of capacity with cycling.

The voltage–composition behavior for samples deposited onto heated substrates (Fig. 5) shows a peculiar behavior. The data are strongly dependent on the sample history. Fig. 5 presents the data for samples deposited at identical conditions, but submitted to different procedures before cycling. One of the samples was cycled after an initial rest period of 16 h in open circuit (therein called treatment 1). The corresponding voltage–composition curve is shown in Fig. 5a. An initial abrupt potential decrease from open circuit potential up to $\sim$1.8 V versus Li^+/Li is followed by a potential increase to $\sim$1.9 V versus Li^+/Li and a well-defined plateau that persist till an reaction level of $\sim$4 lithium ions per mole of compound.

A second process follows, and a second plateau shows up at $\sim$1.45 V versus Li^+/Li. This process corresponds to a lithium uptake of 1.0 lithium ions per mole of compound. The

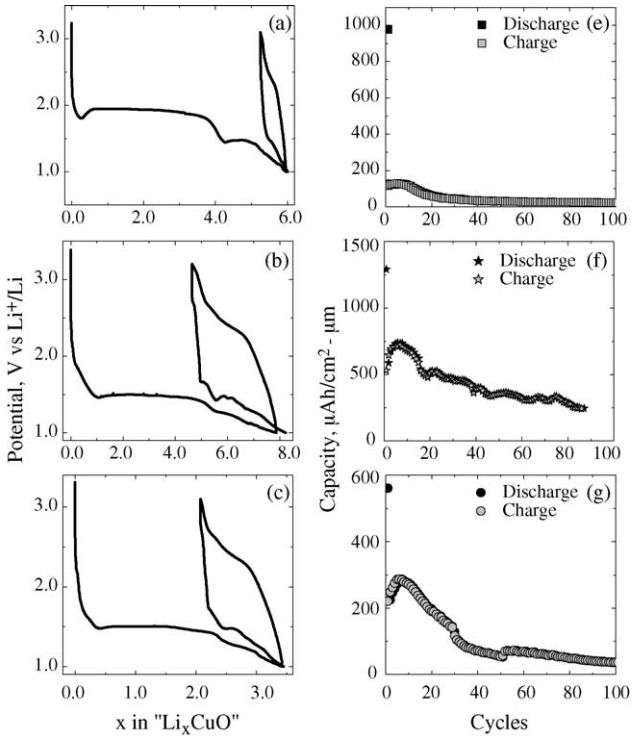

Fig. 5. Voltage–composition curve for samples deposited onto heated substrate. (a) Sample cycled after an initial rest period of 16 h in open circuit (treatment 1). (b) Electrochemical cycling initiated just after sample immersion in the electrolyte (treatment 2) (c) Sample submitted to an Ar jet before immersion in the electrolyte. The electrochemical cycling was initiated just after sample immersion (treatment 3). (e–g) Corresponding capacities curves.

overall process till 1.0 V versus Li+/Li shows that this sample reacts with 6.0 lithium ions per mole of compound, corresponding to a capacity of 979 $\mu Ah\,cm^{-2}\,\mu m^{-1}$ ($\sim$2 $Ah\,g^{-1}$). The electrochemical cycling for the second sample was initiated just after sample immersion in the electrolyte (treatment 2). The curve (Fig. 5b) presents the main plateau at $\sim$1.5 V versus Li^+/Li, and the overall process till 1.0 V versus Li^+/Li shows that this sample reacts with 7.0 lithium ions per mole of compound. The third sample was submitted to a gentle Ar jet before immersion in the electrolyte, and the electrochemical cycling was initiated just after sample immersion (treatment 3). The voltage–composition curve (Fig. 5c) also presents the main plateau at $\sim$1.5 V versus Li^+/Li, but the overall process till 1.0 V versus Li^+/Li shows that this sample reacts with 3.5 lithium ions per mole of compound.

Fig. 5 (right side) shows the behavior of the capacity on cycling. The initial capacity depends on the sample history. An important capacity loss is observed after the initial cycle, but for samples submitted to treatment 2 and 3 an increase is observed till the sixth cycle, followed by a decrease. The RBS data did not indicated any bulk contamination, so the distinct behavior of the samples can be attributed to surface contaminations, either in the transport from the samples from the deposition system to the dry box, or due to organic vapors present inside the dry box. Large irreversible capacity during the first cycle may be caused by formation of solid electrolyte interphase (SEI) [21]. The formation of the SEI is dependent upon the electrode material, the cycling history, and the type of electrolyte solution. If a compact film is formed it can prevents further reaction and a stable cycling is observed. If this is not the case, the irreversible reaction continues on each subsequent discharge. The observed behavior for our samples is consistent with the SEI formation, although potential values lower than 1 V versus Li^+/Li were not attained in the present work. Experimental capacity values higher than the theoretical ones (CuO/Cu reduction process) have been previously observed for materials in thin film form [5].

The stabilized capacity values attained for these kind of electrodes, for all treatments, are higher than for the samples deposited without intentional heating of the substrates, and suitable for use in lithium-ion microbatteries.

4. Conclusions

Nanoparticulated CuO thin films were deposited by reactive dc sputtering at low power, and the electrochemical behavior concerning lithium reactions was investigated. Samples deposited onto heated substrates were amorphous, and presented the best capacity behavior. The attained values demonstrate the potentiality of the use of these materials in lithium-ion microbatteries.

Acknowledgements

Thanks are due to Dr. A. Lourenço and Dr. M. Kleinke for help in the experiments.

References

[1] P. Podhajecky, B. Scrosati, J. Power Sources 16 (1985) 309–317.
[2] P. Poizot, S. Laruelle, S. Grugeon, L. Dupont, J.-M. Tarascon, Nature 407 (2000) 496–499.
[3] J.-M. Tarascon, M. Armand, Nature 414 (2001) 359–367.
[4] B. Laik, P. Poizot, J.-M. Tarascon, J. Electrochem. Soc. 149 (2002) A251–A255.
[5] J.M. Luis Sanchez, F. Martýn, R. Jose, Ramos-Barrado, M. Sanchez, Electrochim. Acta 49 (2004) 4589–4597.
[6] S. Ghosh, D.K. Avasthi, P. Shah, V. Ganesan, A. Gupta, D. Sarangi, R. Bhattacharya, W. Assmann, Vacuum 57 (2000) 377–385.
[7] J.A. Thornton, J. Vac. Technol. A 4 (1986) 3059–3065.
[8] RUMP/GENPLOT, Computer Graphics Service, 2002.
[9] S. Maroie, G. Haemers, J.J. Verbist, Appl. Surf. Sci. 17 (1984) 463–467.
[10] http://www.lasurface.com.br/, 2004.
[11] L.H. Ghijsen, J. Tjeng, J. Vanelp, H. Eskes, J. Westrink, G.A. Sawatzky, M.T. Czyzyc, Phys. Rev. B 38 (1988) 11322–11330.
[12] E. Cano, J.M. Bastidas, J.L. Pólo, N. Mora, J. Electrochem. Soc. 148 (2001) B431–B437.
[13] A. Satta, D. Shamiryan, M.R. Baklanov, C.M. Whelan, Q.T. Le, G.P. Beyer, A. Vantomme, K. Maex, J. Electrochem. Soc. 150 (2003) G300–G306.

[14] J.F. Moulder, W.F. Stickle, P.E. Sool, K.D. Bomber, Handbook of X-ray Photoelectron Spectroscopy, Perkin-Elmer, Eden Prairie, 1992.
[15] S. Grugeon, S. Laruelle, R. Herrera-Urbina, L. Dupont, P. Poizot, J.-M. Tarascon, J. Electrochem. Soc. 148 (2001) A285–A292.
[16] P. Novák, Electrochim. Acta 30 (1985) 1687–1692.
[17] A. Débart, L. Dupont, P. Poizot, J.-B. Leriche, J.M. Tarascon, J. Electrochem. Soc. 148 (2001) A1266–A1274.
[18] J. Svensson, C.G. Granqvist, Appl. Opt. 24 (1985) 2284–2285.
[19] A. Hartridge, M. Ghanashyam Krishna, A.K. Bhattacharya, A. Attia, J.R. Owen, Solid State Ionics 144 (2001) 287–293.
[20] S. Ray, R. Banerjee, N. Basu, A.K. Batabyal, A.K. Barua, J. Appl. Phys. 74 (1983) 3497–3501.
[21] D. Aurbach, A. Zaban, Y. Ein-Ein, I. Weissman, O. Chusid, B. Markovsky, M. Levi, E. Levi, A. Schechter, E. Granot, J. Power Sources 68 (1997) 91–98.